

Comparing Brain Amyloid Deposition, Glucose Metabolism, and Atrophy in Mild Cognitive Impairment with and without a Family History of Dementia

Lisa Mosconi^{a,b,c,*}, Randolph D. Andrews^{a,b}, Dawn C. Matthews^{a,b,*} and For the Alzheimer's Disease Neuroimaging Initiative (ADNI)

^a*Abiant Inc, Grayslake, IL, USA*

^b*ADM Diagnostics, Chicago, IL, USA*

^c*New York University School of Medicine, New York, NY, USA*

Handling Associate Editor: Benedetta Nacmias

Accepted 4 February 2013

Abstract. This study compares the degree of brain amyloid- β ($A\beta$) deposition, glucose metabolism, and grey matter volume (GMV) reductions in mild cognitive impairment (MCI) patients overall and as a function of their parental history of dementia. Ten MCI with maternal history (MH), 8 with paternal history (PH), and 24 with negative family history (NH) received ^{11}C -PiB and ^{18}F -FDG PET and T1-MRI as part of the Alzheimer's Disease Neuroimaging Initiative. Statistical parametric mapping, voxel based morphometry, and Z-score mapping were used to compare biomarkers across MCI groups, and relative to 12 normal controls. MCI had higher PiB retention, hypometabolism, and GMV reductions in Alzheimer-vulnerable regions compared to controls. Biomarker abnormalities were more pronounced in MCI with MH than those with PH and NH. After partial volume correction of PET, $A\beta$ load exceeded hypometabolism and atrophy with regard to the number of regions affected and magnitude of impairment in those regions. Hypometabolism exceeded atrophy in all MCI groups and exceeded $A\beta$ load in medial temporal and posterior cingulate regions of MCI MH. While all three biomarkers were abnormal in MCI compared to controls, $A\beta$ deposition was the most prominent abnormality, with MCI MH having the greatest degree of co-occurring hypometabolism.

Keywords: Alzheimer's disease, amyloid, family history, ^{18}F -fluorodeoxyglucose (FDG), glucose metabolism, magnetic resonance imaging, mild cognitive impairment, positron emission tomography (PET) imaging, Pittsburgh Compound B

Supplementary data available online: <http://dx.doi.org/10.3233/JAD-121867>

INTRODUCTION

Alzheimer's disease (AD) is an age-related neurodegenerative disease and the most common form of dementia. Many clinical studies indicate that by the time patients come in for diagnosis, the amount of irreversible brain damage that may have already occurred

*Correspondence to: Dr. Lisa Mosconi, New York University School of Medicine, 145 East 32nd Street, 5th floor, New York, NY 10016, USA. Tel.: +1 212 263 3255; Fax: +1 212 263 3270; E-mail: lisa.mosconi@nyumc.org; Dawn C. Matthews, ADM Diagnostics LLC, 10 West 35th St., Suite 10F4-2, Chicago, IL 60016. Tel.: +847 707 0370, Fax: +847 223 5018, E-mail: dmatthews@admdx.com.

hinders treatment potential. Effective interventions, as they become available, ideally would be implemented in at risk individuals before symptoms occur.

Mild cognitive impairment (MCI) is characterized by subjective memory impairment that can be objectively verified, while activities of daily living are preserved and the diagnostic criteria for dementia are not fulfilled [1]. MCI, especially its amnesic type, is considered as a prodrome for AD with an annual conversion rate of 10 to 15% of MCI to AD versus a rate of 1 to 2% in normal elderly [2]. Amnesic MCI patients present with AD-specific patterns of brain abnormalities relative to healthy controls. These include increased brain fibrillar amyloid- β (A β) deposition on carbon-11-labelled (N-Methyl)2-(4'-methylaminophenyl)-6-hydroxybenzothiazole (i.e., Pittsburgh compound B, PiB) positron emission tomography (PET) [3–14], reduced glucose metabolism on 2-[¹⁸F]fluoro-2-Deoxy-D-glucose (FDG)-PET [15–20], and increased atrophy on magnetic resonance imaging (MRI) [18, 21–24]. The genetic factors, if any, underlying these brain abnormalities are currently unknown.

While rare genetic mutations have been identified among the early-onset forms of AD, the genetics of the more common forms of late-onset AD (LOAD), which comprises 99% of the AD population after the age of 60, remain elusive. After advanced age, having a parent affected by LOAD is the most significant risk factor for developing the disease [25, 26], and genetically mediated risk is evident from the familial aggregation of many LOAD cases [27]. PET studies of cognitively normal elderly with and without a first degree family history of LOAD have shown that those with an AD-affected mother have increased PiB uptake, reduced glucose metabolism on FDG-PET, and increased atrophy compared to those with an AD-father and those with negative family history [28–34]. As all of these individuals were cognitively normal, the clinical consequence of biomarker abnormalities remains unclear. The only published biomarker study that investigated the effects of having a family history in MCI used MRI to show that MCI with maternal history of dementia had smaller hippocampal volumes and greater 12-month atrophy rates than MCI with negative maternal history [35].

There are currently no studies that have compared the degree of biomarker abnormalities in the same MCI patients, and no studies that examined A β or FDG-PET measures in MCI as a function of their family history of dementia or AD. The goal of the present multi-modality study with brain PiB-PET, FDG-PET,

and MRI was to use voxel-based analysis techniques, such as statistical parametric mapping, voxel-based morphometry, and voxel-wise Z-score mapping, to simultaneously examine and compare the degree of fibrillar A β deposition, glucose metabolism, and gray matter volume reductions in MCI patients with and without a parental history of dementia, and to test whether there are parent-of-origin effects.

METHODS

Subjects

Data used in this study were obtained from the Alzheimer's disease Neuroimaging Initiative (ADNI) database (<http://adni.loni.ucla.edu/>). ADNI is a longitudinal multisite study of normal elderly, amnesic MCI, and AD subjects. MRI and clinical/psychometric assessments are performed at least annually, and other measures including FDG- and PiB-PET have been acquired on a subset of subjects (see <http://www.adni-info.org/>) [36]. This study focused on MCI patients. Briefly, MCI subjects had Mini Mental State Exam (MMSE) scores in the 24–30 range, a memory complaint verified by an informant, objective memory impairment on Wechsler Memory Scale/Logical Memory II test, and Clinical Dementia Rating (CDR) = 0.5 with preservation of general cognition and functional activities of daily living, and did not meet criteria for AD [37–39] (<http://adni.loni.ucla.edu/data-samples/clinical-data/>). Participants were 55–90 years old at the time of enrollment. Subjects were excluded if they refused or were unable to undergo MRI, had other neurological disorders, active depression, or history of psychiatric diagnosis, alcohol, or substance dependence, less than 6 years of education, or were not fluent in English or Spanish. Other grounds for exclusion were residence in a skilled nursing facility, use of psychoactive medications other than certain antidepressants, warfarin, or investigational agents. Written informed consent was obtained from all participants according to Institutional Review Boards regulations at each participating center.

In order to be included in this study, MCI patients had to have MRI, PiB, and FDG scans acquired at the same time point and complete family history information. Subjects were stratified based on their family history of dementia collected through self-report, and only MCI with either maternal (MH) or paternal history of dementia (PH) and controls with negative family history (NH) were included in this study. Twelve

cognitively normal (NL) elderly with NH, no memory complaints, objective memory performance in the normal range, CDR=0 and MMSE 28–30 [37, 38], and who retained a diagnosis of normal cognition for at least 2 years after brain imaging were included as a control group.

Brain imaging

Acquisition

A detailed description of FDG and PiB PET acquisition is found at <http://www.adni-info.org/>. For FDG-PET, a 30-min emission scan, consisting of six 5-min frames, was acquired starting 30 min after the intravenous injection of 5 mCi of 18F-FDG, as the subjects, who were instructed to fast for at least 4 h prior to the scan, lay quietly in a dimly lit room with their eyes open and with minimal sensory stimulation. ^{11}C -PiB with minimum 90% radiochemical purity and minimum specific activity of 300 Ci/mmol was synthesized as outlined by [40]. Subjects were injected with 15 mCi PiB. Scanning started 50 min post-injection and lasted 20 min. Data were corrected for radiation-attenuation and scatter using transmission scans or X-ray CT, and reconstructed using reconstruction algorithms specified for each type of scanner [41] (<http://adni.loni.ucla.edu/data-samples/pet/>).

Image processing

All image data was obtained from the ADNI database at the highest level of pre-processing available. For baseline T1 MRI images, this includes images that are corrected for gradient non-linearity, B1 (coil) non-uniformity correction, and histogram peak sharpening (<http://adni.loni.ucla.edu/data-samples/mri/>). For PET scans, this includes the late uptake 30–60 min post injection summed FDG images and 50–70 min summed PiB images, i.e., an average of co-registered frames that are intensity normalized, resliced to uniform voxel size of $1.5 \times 1.5 \times 1.5$ mm and uniform resolution based on scanner-specific smoothing kernels to ensure an isotropic spatial resolution of 8 mm full-width-at-half-maximum (FWHM) [41] (<http://adni.loni.ucla.edu/data-samples/pet/>). Additionally, within the ADNI framework, PiB scans for each subject are co-registered to the subject's first FDG-PET using the Normalized Mutual Information (NMI) routine implemented in Statistical Parametric Mapping (SPM8) [42, 43]. Standardized uptake value ratios (SUVR) are generated for PiB

scans by normalizing PiB uptake by cerebellar grey matter uptake on a voxel wise basis [44] (<http://adni.loni.ucla.edu/methods/pet-analysis/>).

After downloading, images underwent further processing at our center. For each subject, the corresponding FDG-PET, PiB-PET, and MRI scan were co-registered using NMI and SPM8. The resultant co-registered MRI was partitioned into grey matter (GM), white matter (WM), and cerebrospinal fluid (CSF) segments and normalized to Montreal Neurological Institute (MNI) space by high-dimensional warping (DARTEL) with the standard template included in the VBM8 toolbox [42, 43]. The subject-specific transformation matrixes obtained from these operations were applied to spatially normalize each MRI-coregistered FDG and PiB scan (final voxel size $2 \times 2 \times 2$ mm). Spatially normalized PET images were smoothed with a 10 mm FWHM gaussian filter and examined for voxel-wise effects with SPM (see below).

FDG and PiB-PET scans were corrected for partial volume effects (PVE) using a 3-segments voxel-by-voxel method (GM versus WM versus CSF) [45] implemented in PMOD (version 3.2; PMOD Technologies Ltd. 2011). Regional atrophy may bias PET measurements since age and disease-related atrophy might lower the estimated metabolism and A β load because of PVE, which are caused by the inclusion of metabolically inactive CSF spaces and spillover from WM [45, 46]. PVE-correction was performed to ascertain whether a true reduction in glucose metabolism and an increase in amyloid load per gram brain tissue occur in MCI. PVE-corrected scans were coregistered onto their respective MRI, spatially normalized and smoothed using the same procedures as with raw images.

Voxel-based morphometry (VBM) within the SPM8 suite [42, 43] was used to evaluate brain morphometry on MRI on a voxel-wise basis. A custom template and tissue probability maps (TPMs) were created in SPM8 using the T1-weighted 3D MRI scans from all subjects in the study. The custom template and TPMs were created by first normalizing and segmenting the MRI scans using the unified segmentation model in SPM8 with the standard MNI template and TPMs, followed by a clean-up step which uses a hidden Markov random field (HMRF) model to increase the accuracy of the individual subject TPMs, and finally averaging the normalized subject TPMs. All subject images were then normalized and segmented using the unified segmentation model and the custom TPMs, followed by the HMRF clean-up step. Jacobian modulation was applied to compensate for the effect of spatial

normalization and to restore the original absolute grey matter volumes (GMV) in the segmented grey matter images. These modulated images were then smoothed with an 8-mm FWHM smoothing kernel. Additionally, total GM, WM, CSF, and intracranial volumes (TIV) were calculated in cubic centimeters using the normalized tissue maps for each study subjects and separately analyzed.

Statistical analysis

SPSS v.19 (SPSS Inc., 2011) and Statistical Parametric Mapping (SPM8) were used for statistical analysis. Differences in clinical and demographical measures between groups (NL versus MCI NH versus MCI PH versus MCI MH) were examined with the General Linear Model (GLM) with *post-hoc* LSD tests and χ^2 tests, as appropriate.

Comparing biomarkers across groups

The following comparisons were performed: (a) all MCI patients versus controls; (b) each MCI family history group versus controls; (c) each MCI family history group against each other. A full factorial model with four groups (NL versus MCI NH versus MCI PH versus MCI MH) was used to test for regional differences in PiB, FDG, and GMV scans across groups using *post-hoc* linear *t*-contrasts within the GLM framework of SPM8. Other possible risk factors for LOAD, such as age, gender, education, and *APOE* genotype were examined as covariates. Whole-brain FDG measurements were computed using the *spm_global* routine and used to normalize the scans for the individual variation in whole-brain metabolism. This is a common procedure to highlight regional hypometabolism which has been previously used in similar study populations [32, 33]. Relative threshold masking was set at 80% of the mean global value, on the basis that any voxel with values in the bottom 20% of metabolic activity would reflect WM and metabolically inactive CSF spaces. This procedure restricts analysis to tracer uptake in gray matter structures [47]. For PiB-PET analysis, as a result of the cerebellar normalization of PiB data, no proportional scaling or grand mean scaling was performed. For VBM-MRI analysis, modulated outputted GMV images are corrected for non-linear warping, effectively globally scaling data for TIV. Therefore, no proportional scaling or grand mean scaling was performed. PVE-corrected FDG- and PiB-PET images were compared across groups using the same procedures as above.

Comparing biomarkers to each other

Spatially normalized MRI and PVE-corrected PET images were used to create Z-score maps for each patient against the 12 NL controls [$Z = (\text{patient individual value} - \text{control mean}) / \text{control standard deviation}$], for each modality (see [48] for a similar approach). The creation of Z-score maps offers a direct comparison of the degree of A β load (PiB), hypometabolism (FDG), and GMV loss (MRI). Positive PiB Z scores reflect increased A β load and negative FDG and GMV Z scores reflect deficits relative to controls. In order to compare Z maps from different modalities in a manner where disease progression was a positive value across modalities, FDG and GMV Z score images were multiplied by (-1) . Individual PiB, FDG, and GMV Z-score maps were then examined in an SPM paired *t*-test analysis, with one group and two Z score images per subject (PiB versus FDG, PiB versus MRI, FDG versus MRI). This analysis was performed first for the entire MCI group, and then for each family history group (NH, PH, MH). As Z scores are standardized values, no proportional scaling or grand mean scaling was performed. Both contrasts were assessed for each modality comparison (for example, Z-FDG > Z-MRI and Z-MRI > Z-FDG).

For all analyses, a GM mask including only voxels with probability of being GM >90% was used as an explicit mask to analyze data exclusively within the same GM voxels for all modalities [42, 43]. Since the brain regions showing differences in MCI versus controls, and in association with AD FH have been previously identified by several studies [4–8, 10, 13, 15, 16, 19, 21, 23, 28, 30, 33, 35, 49, 50], results were examined at $p \leq 0.001$, uncorrected for multiple comparisons (cluster extent >20 voxels). Additionally, in order to take into account group differences in sample size (N), results were re-examined after adjusting the p value according to the formula $p' = 0.05/N$ [31, 51–54]. This resulted in exploratory thresholds of $p' \leq 0.002$ for NH, $p' \leq 0.005$ for MH, and $p' \leq 0.006$ for PH. Anatomical location of brain regions showing significant effects was described using Talairach and Tournoux coordinates, after conversion from the MNI to the Talairach space using linear transformations [<http://www.mrc-cbu.cam.ac.uk/Imaging/>]. PiB, FDG, and GMV measures, as well as Z score values, were sampled from clusters of voxels showing significant effects using the SPM-compatible MarsBar tool (release 0.43, <http://marsbar.sourceforge.net/>) for descriptive purposes.

RESULTS

Subjects

A total of 42 MCI patients fulfilled our inclusion criteria, including 10 MH, 8 PH, and 24 NH. The parents of 7/10 (70%) MH subjects and 5/8 (63%) PH subjects had a specific diagnosis of AD. MCI family history groups were comparable for age, gender, education, MMSE, and *APOE* status (Table 1). As per study design, NL controls were of similar demographic characteristics as MCI patients (Table 1).

PiB-PET differences across groups

Compared to NL controls, the entire MCI group showed higher PiB retention, reflecting increased amyloid load, in middle and lateral frontal, parietal, temporal, posterior cingulate cortex (PCC), precuneus and striatum, bilaterally, and to a lesser extent in occipital cortex and thalamus ($p < 0.001$; Fig. 1A). Comparison of each MCI family history group to controls showed no regions of increased PiB retention in MCI NH, and increased PiB retention in PCC, precuneus, frontal, parietal, and temporal cortices of MCI MH and PH groups ($p < 0.001$, Fig. 1A). PiB deposition was more widespread in MH than in PH (Fig. 1A).

Direct comparison of MCI groups confirmed that the MH group had increased PiB retention in PCC, precuneus, and temporal cortex, bilaterally, compared to NH, and in PCC and precuneus compared to PH ($p \leq 0.001$, Fig. 2). Quantitatively, PiB SUVRs were

$31 \pm 10\%$ higher in MH relative to NH (range 18% in PCC to 40% in temporal cortex) and 19% higher in PCC of MH relative to PH. Additionally, at a sample size-adjusted exploratory threshold of $p' < 0.005$, the MH group showed additional clusters of increased PiB retention in superior temporal gyrus (BA 22, $x = 59$, $y = -53$, $z = 8$, $K_e = 80$ voxels, $Z = 2.5$) and superior parietal lobule (BA 7, $x = 31$, $y = -60$, $z = 45$, $K_e = 65$ voxels, $Z = 2.6$, $p's = 0.004$) compared to NH (Fig. 2). Statistical parametric maps showed mild PiB retention increases in parieto-temporal and frontal regions of MH compared to PH, which did not reach statistical significance (Fig. 2).

There were no differences between PH and NH at $p \leq 0.001$. At a sample size-adjusted exploratory threshold of $p' < 0.006$, PH showed increased PiB retention in precuneus (9%, BA 7, $x = -18$, $y = -54$, $z = 56$, $K_e = 85$ voxels, $Z = 3.0$, $p' = 0.004$) compared to NH. There were no clusters of increased PiB retention in PH compared to MH at any probability threshold. Results remained unchanged correcting for age, gender, education, and *APOE* status.

PVE correction had the general effect of increasing PiB retention in all MCI groups. After PVE correction, the NH group still showed no differences compared to NL, while MH and PH groups showed higher PiB retention in AD-regions compared to NL and to MCI NH ($p < 0.001$, Supplementary Figure 1; available online: <http://www.j-alz.com/issues/35/vol35-3.html#supplementarydata01>). Although PiB retention appeared to be more extensive in MCI MH than PH (Supplementary Figure 1), the differences did not reach

Table 1
Clinical and MRI volume measures in MCI patients as a function of their family history of dementia and cognitively normal (NL) controls

	NL	MCI		
		NH	PH	MH
<i>n</i>	12	24	8	10
Age (y)	76+5	76(8)	72(10)	72(7)
Gender (female/male, % female)	3/9 (25%)	8/16 (33%)	2/6 (25%)	5/5 (50%)
Education (y)	16(3)	16(2)	17(2)	15(3)
Mini Mental State Examination	29(1)	27(2)	27(3)	28(2)
<i>APOE</i> ($\epsilon 4$ non-carriers/carriers, % carriers)	9/3 (25%)	12/12 (50%)	2/6 (75%)	4/6 (60%)
MRI measures (cm ³)				
Grey matter volume	532(60)	514(78)	544(88)	527(42)
<i>Covariate adjusted</i>	537(52)	522(72)	539(73)	514(72)
White matter volume	598(50)	583(74)	622(99)	563(57)
<i>Covariate adjusted</i>	599(42)	583(79)	623(80)	562(80)
Cerebrospinal fluid volume	276(34)	306(46)	301(39)	282(37)
<i>Covariate adjusted</i>	274(30)	301(40)	306(40)	291(40)
Total intracranial volume	1406(125)	1404(152)	1468(198)	1371(114)
<i>Covariate adjusted</i>	1410(136)	1405(162)	1469(165)	1366(134)

Values are mean (standard deviation). Covariate-adjusted values are in *italic* (covariates are age, gender, education, and *APOE* status). MH, maternal history of dementia; NH, negative history of dementia; PH, paternal history of dementia.

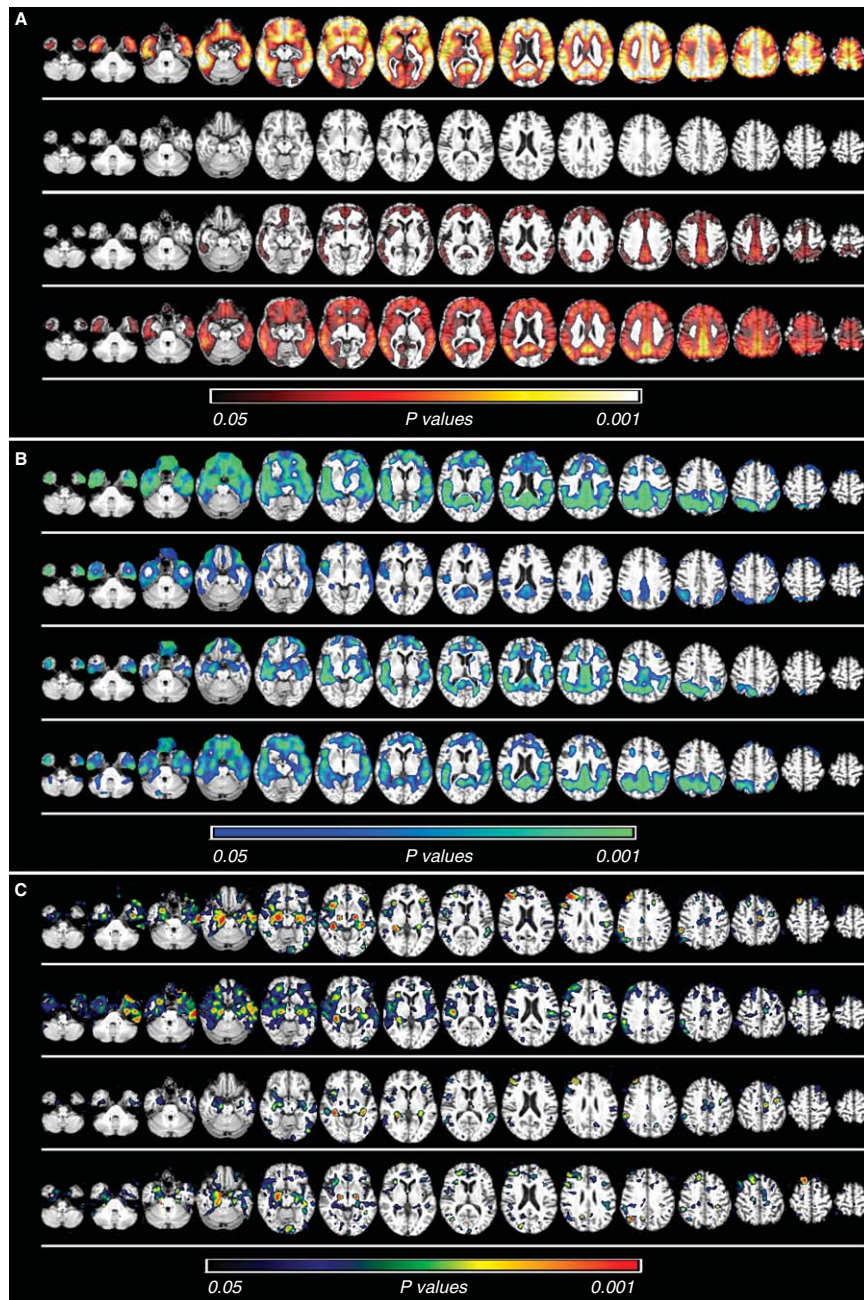


Fig. 1. Brain regions showing differences in brain biomarkers between normal controls and MCI family history groups. A) Brain regions showing differences in brain fibrillar amyloid load on PiB-PET. *First row*: Increased PiB retention in the entire MCI group compared to controls. *Second row*: Increased PiB retention in MCI with negative family history of dementia (NH) compared to controls. *Third row*: Increased PiB retention in MCI with a paternal history of dementia (PH) compared to controls. *Bottom row*: Increased PiB retention in MCI with a maternal history of dementia (MH) compared to controls. B) Brain regions showing differences in brain glucose metabolism on FDG-PET. *First row*: Reduced metabolism in the entire MCI group compared to controls. *Second row*: Reduced metabolism in MCI NH compared to controls. *Third row*: Reduced metabolism in MCI PH compared to controls. *Bottom row*: Reduced metabolism in MCI MH compared to controls. C) Brain regions showing differences in brain grey matter volumes (GMV) on MRI. *First row*: Reduced GMV in the entire MCI group compared to controls. *Second row*: Reduced GMV in MCI NH compared to controls. *Third row*: Reduced GMV in MCI PH compared to controls. *Bottom row*: Reduced GMV in MCI MH compared to controls. Statistical parametric maps indicating regions of (A) increased PiB retention, reflecting higher amyloid load, (B) reduced FDG-PET uptake, reflecting reduced brain glucose metabolism, and (C) reduced GMV, reflecting increased brain tissue loss (i.e., atrophy) are represented on different color coded scales and superimposed onto a spatially normalized MRI template image.

statistical significance, with or without correcting for the same covariates as above.

FDG-PET differences across groups

Compared to NL controls, the entire MCI group showed reduced FDG uptake, reflecting reduced brain glucose metabolism, in PCC, precuneus, parietal, medial, and lateral temporal cortex, medial, lateral, and orbitofrontal regions, bilaterally ($p < 0.001$; Fig. 1B). When each MCI group was compared to controls, FDG uptake reductions were more widespread and pronounced in MH than in PH and NH (Fig. 1B).

Direct comparison of MCI groups confirmed this effect (Fig. 2). The MH group had reduced metabolism in inferior parietal lobule and middle frontal cortex compared to NH (15% and 17%, respectively) and in superior temporal cortex compared to PH (9%, $p \leq 0.001$). At a size-adjusted threshold of $p' < 0.005$, the MH group showed additional regional hypometabolism in frontal lobe (9% BA 25, $x = 11$, $y = 28$, $z = -12$, $Ke = 66$, $Z = 2.6$, $p = 0.004$) and PCC/precuneus (10% BA 31, $x = -14$, $y = -57$, $z = 29$, $Ke = 364$, $Z = 2.5$, $p = 0.005$) compared to NH, and in precuneus compared to PH (10% BA 7, $x = 21$, $y = -54$, $z = 57$, $Ke = 111$, $Z = 2.4$, $p = 0.005$). There were no differences between PH and NH, and no regions showing metabolic reductions in PH compared to MH, at any probability threshold. Results remained substantially unchanged correcting for age, gender, education, and *APOE* status.

PVE correction had the general effect of increasing metabolic values in all MCI groups, which left group differences largely unchanged in terms of the regional distribution of hypometabolism ($p < 0.001$, Supplementary Figure 2).

Grey matter volume differences across groups

On VBM analysis, the entire MCI group showed reduced GMV, reflecting increased atrophy, in medial temporal lobe regions, including hippocampus and parahippocampal gyrus, bilaterally, and in prefrontal cortex compared to NL controls ($p < 0.001$; Fig. 1C). GMV reductions were overall comparable across MCI family history groups compared to NL (Fig. 1C), and there were no differences across MCI groups at $p < 0.001$. At a sample size-adjusted exploratory threshold of $p' < 0.005$, MH showed reduced GMV compared to NH in the left precuneus (BA 7, $x = -2$, $y = -79$, $z = 40$, $Ke = 41$, $Z = 3.1$, $p = 0.002$, Fig. 2). There were no regions showing GMV differences

between MH and PH, or PH and NH, at any probability threshold.

There were no group differences for total GM, WM, and CSF volumes obtained by VBM processing, with and without controlling for age, gender, education, and *APOE* status (Table 1).

Comparisons between modalities

PiB versus FDG-PET

Comparison of PVE-corrected PiB and FDG-PET Z-scores showed significant differences for both contrasts, i.e., $A\beta$ load > hypometabolism and hypometabolism > $A\beta$ load. Across all MCI subjects, the degree of $A\beta$ load exceeded that of hypometabolism in precuneus, posterior and anterior cingulate cortex, parietal, frontal, orbitofrontal and occipital cortex, and striatum, bilaterally ($p < 0.001$, Fig. 3). This effect was observed in all family history groups, and was more pronounced in MH (mean Z score: PiB = -2.6 versus FDG = -0.5) and PH (PiB = -2.8 versus FDG = -0.2) than in NH (PiB = -1.7 versus FDG = -0.5 , p 's < 0.05; Fig. 3).

The degree of hypometabolism exceeded that of $A\beta$ load in medial and lateral temporal cortex, bilaterally, in the entire MCI sample ($p < 0.001$, Fig. 3). This effect was more pronounced in MH (mean Z score: FDG = -2.5 versus PiB = -0.5) compared to PH (FDG = -1.6 versus PiB = -0.4) and to NH (FDG = -1.9 versus PiB = -0.3 , p 's < 0.05; Fig. 3). Voxel-wise examination of each family history group confirmed that the above effect was largely driven by the MH group, in which hypometabolism exceeded $A\beta$ load in medial and lateral temporal cortices as well as precuneus ($p \leq 0.001$).

PiB versus MRI

Comparison of PVE-corrected PiB-PET and GMV-MRI Z-score images showed significant differences for the $A\beta$ load > atrophy contrast only. Across all MCI subjects, the degree of amyloid load exceeded that of GMV loss (i.e., atrophy) in precuneus, PCC, parietal and temporal cortex, bilaterally ($p < 0.001$; Fig. 3). This effect was observed in all family history groups, and was more pronounced in MH (mean Z score: PiB = -2.4 versus GMV = -0.7) and PH (PiB = -2.5 versus GMV = -1.05) than in NH (PiB = -1.7 versus GMV = -1.0 , p 's < 0.05; Fig. 3).

FDG-PET versus MRI

Comparison of PVE-corrected FDG-PET and GMV-MRI Z-score images showed significant

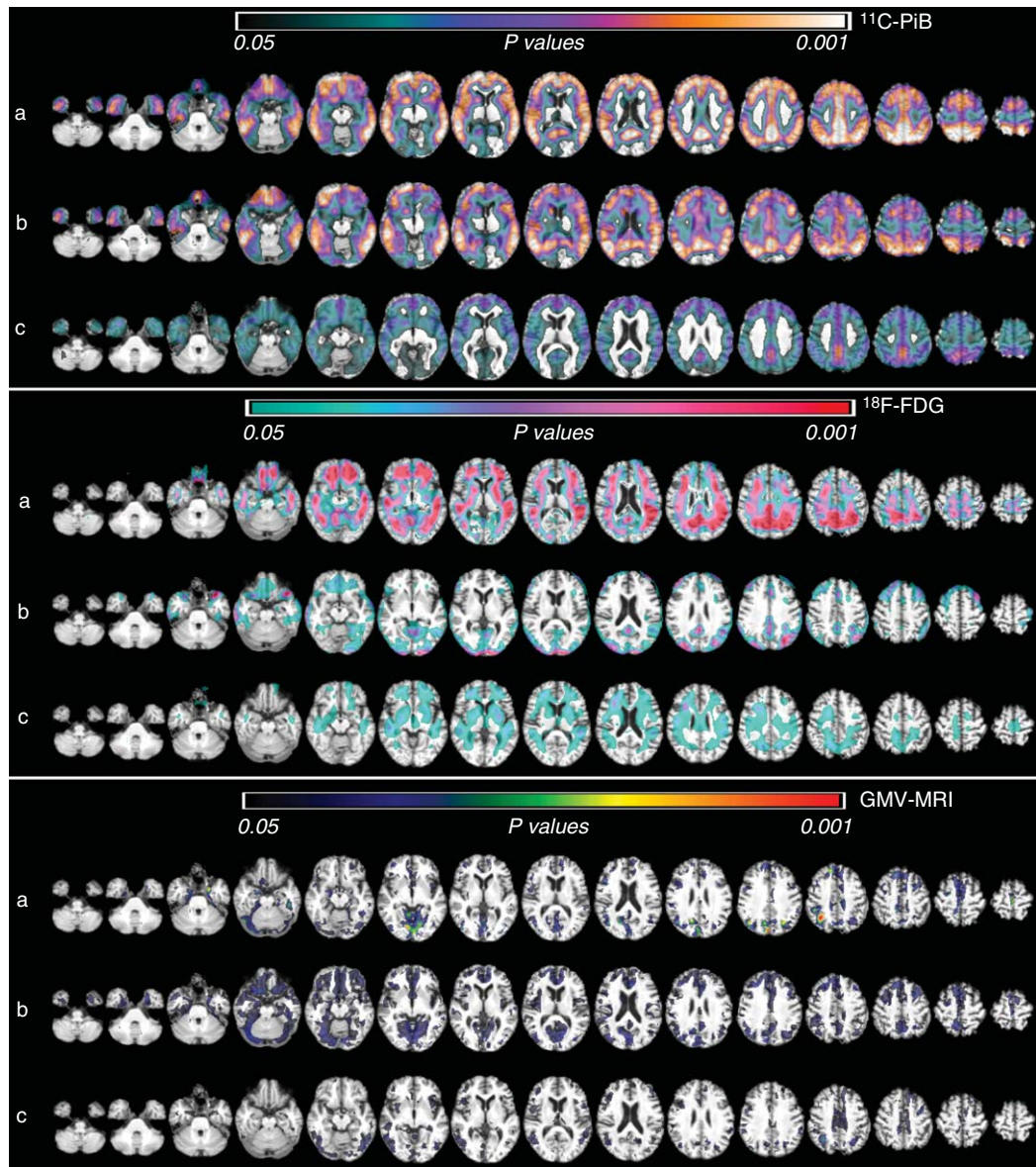


Fig. 2. Brain regions showing biomarkers differences across MCI family history groups. *Top panel:* Fibrillar amyloid load on PiB-PET: a) Increased PiB retention, reflecting higher amyloid load, in MCI MH compared to NH; b) Increased PiB retention in MCI MH compared to PH; c) Increased PiB retention in MCI PH compared to NH. *Middle panel:* Brain glucose metabolism on FDG-PET: a) Reduced FDG uptake, reflecting reduced glucose metabolism, in MCI MH compared to NH; b) Reduced metabolism in MCI MH compared to PH; c) Reduced metabolism in MCI PH compared to NH (no clusters reached statistical significance). *Bottom panel:* Grey matter volumes (GMV) on MRI: a) Reduced GMV, reflecting increasing brain tissue loss (i.e., atrophy) in MCI MH compared to NH; b) Reduced GMV in MCI MH compared to PH (no clusters reached statistical significance); c) Reduced GMV in MCI PH compared to NH (no clusters reached statistical significance). Statistical parametric maps indicating regional biomarkers abnormalities are represented on a color coded scale and superimposed onto a spatially normalized MRI template image. Abbreviations: see legend to Figure 1.

differences for the hypometabolism > atrophy contrast only. Across all MCI subjects, the degree of hypometabolism exceeded that of GMV loss in precuneus, PCC, medial temporal lobes, bilaterally, and inferior temporal cortex of the left hemisphere

($p < 0.001$; Fig. 3). This effect was observed in all family history groups, and was more pronounced in MH (mean Z score: FDG = -2.3 versus GMV = -0.6) than in PH (FDG = -1.6 versus GMV = -1.04) and in NH (FDG = -1.8 versus GMV = -1.1 , p 's < 0.05 ; Fig. 3).

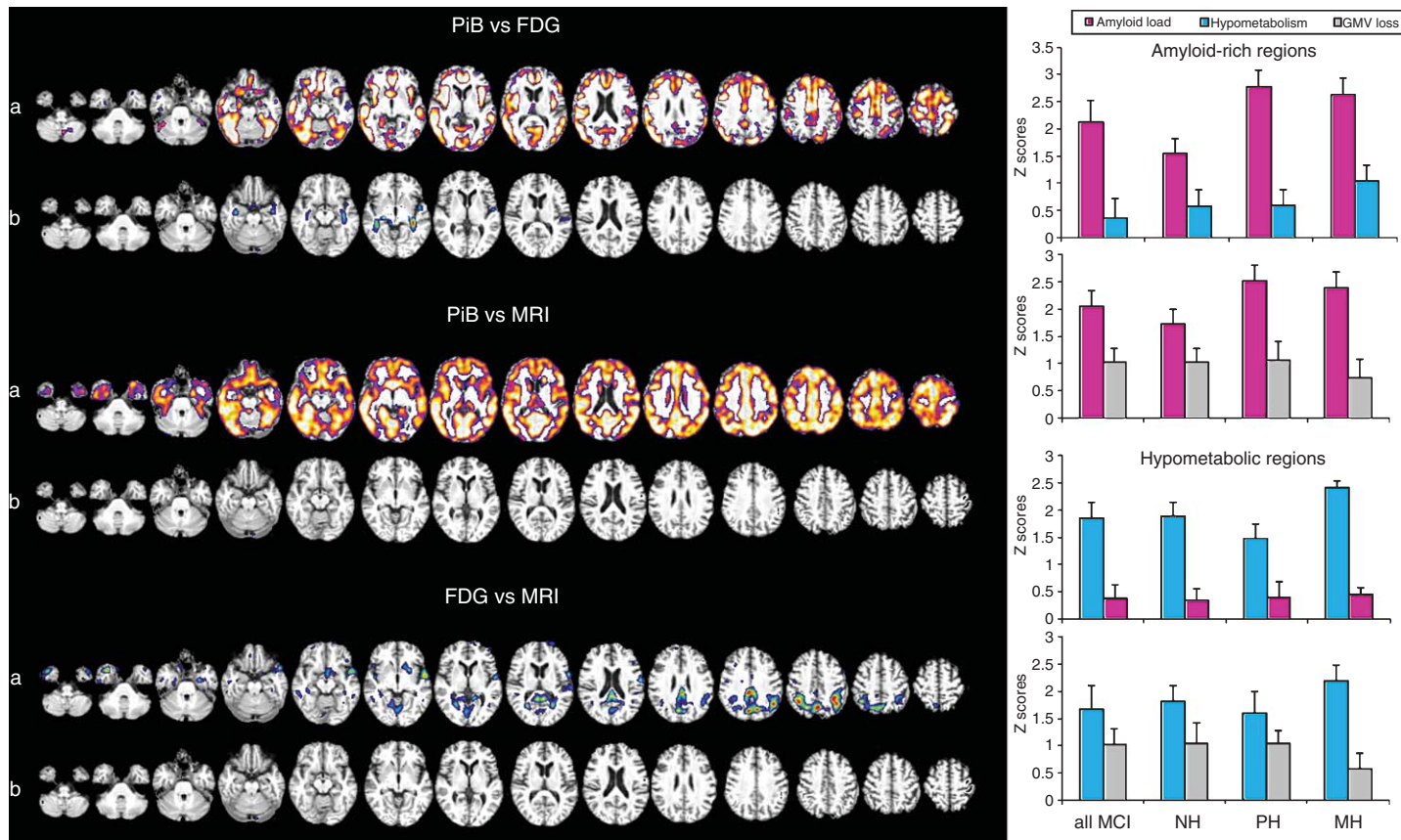


Fig. 3. Comparison of amyloidosis, hypometabolism, and gray matter volume (GMV) loss. Left side of figure: Voxel-based comparisons of Z score images across all MCI subjects. *Top panel:* PiB versus FDG. Statistical parametric maps (SPMs) showing regions in which (a) the degree of amyloid load exceeds that of hypometabolism; and (b) the degree of hypometabolism exceeds that of amyloid load. *Middle panel:* PiB versus MRI. SPMs showing regions in which (a) the degree of amyloid load exceeds that of GMV loss (i.e., atrophy); and (b) the degree of GMV loss exceeds that of amyloid load (no clusters reached statistical significance). *Bottom panel:* FDG versus MRI. SPMs showing regions in which (a) the degree of hypometabolism exceeds that of GMV loss; and (b) the degree of GMV loss exceeds that of hypometabolism (no clusters reached statistical significance). PiB- and FDG-PET scans are corrected for partial volume effects. SPMs are represented on a color coded scale ($0.05 \leq p \leq 0.001$), and superimposed onto a spatially normalized MRI template image. Right side of figure: Mean Z score values extracted from the clusters reaching statistical significance on voxel-based analysis and corresponding to SPMs shown to the left, are plotted for the entire MCI group and for each family history group (NH, PH, MH). Z scores are absolute values. Error bars are SEM.

DISCUSSION

This multi-modality brain PiB-PET, FDG-PET, and MRI imaging study was aimed at characterizing the distribution and comparing the degree of amyloidosis, hypometabolism, and GMV loss (i.e., atrophy) in MCI patients, and as a function of their parental history of dementia. To our knowledge, this is the first report of parental history affecting amyloid deposition and hypometabolism in MCI, and of differences in the degree of amyloidosis, hypometabolism, and GMV loss in MCI patients using either a regions of interest or voxel-wise quantitative comparisons. Our results show that amyloid load exceeds hypometabolism and atrophy in several AD-vulnerable regions of MCI patients, including frontal, parietal, PCC, temporal and occipital cortices, precuneus, and striatum. PiB retention in these regions is consistent with the known distribution of A β plaques observed at postmortem [55, 56]. Additionally, hypometabolism exceeded amyloidosis in MTL, and exceeded atrophy in precuneus, PCC, MTL, and inferior temporal regions. These effects were largely driven by the MCI MH group and were absent or less pronounced in MCI PH and NH groups. There were no regions in which atrophy exceeded amyloid load or hypometabolism.

These results lend support to the hypothetical model of dynamic biomarkers of the AD pathological cascade proposed by Jack et al. [23]. Currently available evidence supports the position that an abnormal processing of A β peptide, ultimately leading to formation of A β plaques in the brain, is the initiating event in AD [57]. After a lag period, which varies from patient to patient, A β deposition would plateau and neuronal dysfunction and neurodegeneration become the dominant pathological processes, with FDG-PET changes preceding MRI changes. Only a few prior studies have tackled the question of which biomarker abnormality is more prominent in AD by comparing FDG-PET to MRI. Results showed that the degree of hypometabolism exceeded that of atrophy in MCI and AD patients [18, 21, 48] as well as in pre-symptomatic, autosomal dominant mutation carriers [58]. Our findings in MCI support these observations and provide further insights into the possible ordering of pathophysiological events by showing that A β deposition exceeds, and therefore possibly precedes, FDG-PET and MRI changes. However, a temporal relationship between biomarkers cannot be reliably determined based on cross-sectional findings. Longitudinal studies are needed to ascertain the dynamic relationship between A β deposition,

neuronal dysfunction, and loss during the progression to AD.

While A β deposition, metabolic impairment, and tissue loss are likely co-occurring phenomena in AD, discrepancies in timing and regional distribution are to be expected, especially in early disease. PiB retention co-localizes with A β plaques [10] and volume loss on MRI reflects local neuronal loss and death [59], while FDG uptake reflects local glucose consumption and synaptic functioning, and is therefore influenced by various factors, including reduced synaptic activity [60], neuronal disruption by A β oligomers and plaques [57], and disconnection between histopathologically affected regions and functionally associated areas [61, 62]. Our results confirmed the previously reported dissociation between A β accumulation and neurodegeneration in MTL [7, 9, 10, 44, 63, 64] as MCI patients, particularly those with MH, showed MTL hypometabolism and atrophy in absence of co-localized PiB retention. This data further indicates that local A β toxicity may not be the only determinant of neuronal dysfunction in early AD, and is consistent with reports of differential susceptibility to A β among different brain regions [5, 23, 65].

Our results revealed parent-gender effects on biomarkers abnormalities in MCI. On PiB-PET, both MCI MH and PH groups showed increased A β deposition compared to NL controls, whereas MCI NH showed no regions of increased A β deposition. Additionally, the MH group showed higher A β load than PH, and hypometabolism on FDG-PET compared to NL controls as well as to MCI PH and NH. There were no GMV differences across MCI groups on MRI. These findings have several implications.

First, the fact that MCI MH and PH patients of similar demographical characteristics show comparable levels of increased A β load indicates that having a first degree family history of dementia may predispose individuals to increased amyloid deposition, reflecting the known increased clinical risk [25–27] and irrespective of which parent is affected. First-degree relatives of affected probands, especially children, are at 4- to 10-fold higher risk for developing dementia as compared to those without [26, 66–68]. The observation that NH MCI did not show significant PiB abnormalities compared to controls supports epidemiological evidence of lower risk for AD. As not all MCI patients progress to an AD diagnosis, our study suggests that MCI NH may represent a sub-group of MCI with lower chance of having AD, and who may therefore be more likely to remain clinically stable over time compared to the other groups.

Second, only MCI MH showed significant hypometabolism compared to NL subjects. The degree to which hypometabolism exceeded that of amyloid load was also greater in MCI MH than in MCI NH and PH. Histology studies have shown that among individuals with A β pathology, those with accompanying neuronal dysfunction are more likely to develop dementia in life than those without [69, 70]. Presence of neurodegeneration, rather than pathology, is best associated with clinical disabilities in AD [71], and measures of brain atrophy and glucose metabolism are more tightly correlated with cognitive performance than the PiB signal [5, 9, 23, 63, 64, 72–74]. Individuals harboring A β burden and neuronal dysfunction are thus at conceivably higher risk for AD-dementia than those showing A β pathology alone [23, 75]. Evidence of co-occurring amyloidosis, hypometabolism, and GMV loss suggests greater risk of decline in MCI MH relative to MCI PH. Epidemiological studies have shown that maternal transmission of AD is associated with higher risk of developing the disease, poorer cognitive performance, and a more predictable age at onset in the offspring relative to paternal transmission [27, 76–79]. Previous PiB- and FDG-PET studies in NL elderly showed that those with MH had amyloidosis and hypometabolism in the same brain regions as clinical AD patients compared to NL PH and controls, while NL PH showed milder A β deposits than MH as compared to controls and no metabolic deficits [30–33]. Our multi-modality results extend to the MCI stage previously reported single modality findings of an association between maternal history and biomarker alterations at the normal stages of cognition, and support the hypothesis that paternal transmission may be associated with lower biological risk [28–30, 33–35, 80, 81]. Altogether, these data indicate that clinical deterioration does not outweigh the effect of MH, as PiB and FDG-PET abnormalities are present in NL as well as in MCI individuals with MH, and to a lesser extent in those with PH [30, 32, 33]. Third, the presence of both A β pathology and hypometabolism in MCI MH indicates that these brain abnormalities developed at younger ages in these subjects. The temporal and causal relationship between A β and glucose dysmetabolism remains to be established. Nonetheless, with all that is known about the mechanisms involved in glucose utilization and maternal inheritance, evidence for early oxidative dysmetabolism in MH suggests transmission through mitochondrial genes, which are entirely maternally inherited in humans and whose expression is known to affect A β production in AD (for review, see [27,

82]). Metabolic abnormalities in MH may be an early, maternally inherited abnormality that increases vulnerability to A β pathology during the aging process. Alternatively, they may be secondary to the toxic effects of A β [57]. Larger samples and longitudinal examinations are necessary to determine whether observed biomarker abnormalities in our MCI patients with family history are predictive of future dementia, to clarify the temporal relationship between biomarkers, and the age at which biomarker changes occur.

MRI studies in NL elderly using VBM techniques reported cortical as well as medial temporal atrophy in NL individuals with MH compared to PH and controls [28, 29, 49]. The present study with VBM showed reduced MTL GMV, encompassing the hippocampal region, in all MCI groups, but no differences across family history groups. These data further suggest that atrophic changes may follow amyloid deposition and hypometabolism, and group differences may become significant at later stages of disease progression. However, a longitudinal MRI study using sophisticated automated hippocampal segmentation and radial distance mapping techniques showed that MCI with positive MH had smaller hippocampal volumes at baseline, and greater 12-month atrophy rates as compared to MCI with negative MH of dementia [35]. The VBM approach performs voxel-wise examinations and as such does not focus on a specific region of interest [42, 43]. It is possible that more accurate delineation of the hippocampus, rather than whole-brain voxel-wise analysis, might have led to different results. Alternatively, a larger sample may be needed to detect structural differences between MCI groups. Andrawis et al. [35] examined 72 MCI with MH and 26 without MH. Our sample was substantially smaller, as we were limited by the need to examine MCI patients with MRI as well as PiB- and FDG-PET. Nonetheless, PiB and FDG differences between groups reached statistical significance, supporting the view that alterations in these biomarkers might be more prevalent than GMV changes in MCI. Additionally, an interaction between maternal history and *APOE* ϵ 4 genotype on MRI measures was previously observed in MCI [35]. Due to the small sample of patients in this study (Table 1), we could not test for interactions between family history and *APOE* status or for correlations between imaging measures and the dose of ϵ 4 allele, as only four subjects were ϵ 4/ ϵ 4 carriers, including two MCI NH, one MCI PH, and one MCI MH. Other studies are warranted to address this important topic.

In ADNI, parental history of dementia is provided by self-report. We chose to use the parental history of dementia variable as opposed to the parental history of AD variable as in some cases the etiology of parental dementia was not recorded. The parents of 12/18 MCI with positive family history had a diagnosis of AD, including 7/10 MH and 5/8 PH. As a similar proportion of MH and PH patients had AD-parents, biomarker differences are unlikely to be driven by one group including more individuals with non-AD dementia than the other. While limited by the small sample, we examined brain imaging measures in MCI patients with a parental history of AD, and found a strong overlap with the remaining MCI for all biomarkers (data available upon request). Additionally, family history questionnaires are known to have good agreement with clinical and neuropathological findings [83]. AD is the most common dementia etiology and is found in about 3/4 dementia cases at postmortem [23]. Nonetheless, our cohort might include patients whose parents had non-AD dementia, such as vascular dementia, Lewy bodies, or frontotemporal dementia. This would lead to inclusion of subjects with lower risk for AD in the family history groups, conservatively reducing power in detecting group differences. As only a portion of MCI patients have underlying AD as the cause of their cognitive impairment, it remains to be determined if MCI MH are more likely to progress to AD than MCI with other family history.

While our sample was too small to include an adequate number of decliners to AD to make this topic a main analysis of our study, all MCI patients had follow-up exams 12 months after the imaging procedures. A total of 14/42 MCI declined to AD 12 months after baseline. These included 4/10 (40%) MCI FHm and 3/8 (38%) MCI FHp, as compared to 7/24 (29%) MCI FH-. One MCI FH- reverted back to a NL diagnosis. While these differences did not reach statistical significance, possibly due to the small samples, these data suggest that having a positive family history may be associated with a higher likelihood of developing AD as compared to having no family history in MCI patients. Our cross-sectional study indicates that MCI with positive family history show more severe PiB and FDG-PET abnormalities than those without, thereby indicating greater vulnerability to AD and possibly, a higher risk of decline. Other studies with larger samples and longer follow ups are needed to specifically examine the rate of decline in MCI as a function of their family history, and to compare imaging measures between decliners and non-decliners as a function of their family history.

Information on AD neuropathology and CSF markers would also be of great interest. The ADNI database includes measures of CSF A β and tau proteins for a sub-set of participants. Of the 54 subjects included in our study, CSF data was available for a total of 22 cases (40%), including four NL controls, ten MCI NH, four MCI PH, and two MCI MH. As only less than half of our subjects had CSF measures at the same time point as the PET scans, and the majority of those individuals have negative family history, we did not include CSF data in the present paper. Our goal was to compare PiB, FDG, and MRI measures in MCI with and without a family history of dementia. Other studies with larger samples are warranted to examine CSF measures together with PET and MRI imaging with respect to MCI patients' family history status.

In the present study, results were examined using voxel-based methods and probability thresholds uncorrected for multiple comparisons. This was due to the fact that, first, we had strong regional *a priori* hypothesis as to which brain areas would show differences between groups. Uncorrected *p* thresholds are appropriate when examination of voxel-wise results is limited to a predefined set of regions of interest, whereas correction for multiple comparisons is necessary when there is no *a priori* hypothesis on which brain regions would show effects of interest, and thus, the goal is to minimize false positives. Additionally, correction for multiple comparisons would have been over-conservative with the small samples included in this study (10 MH and 8 PH). Results were examined using uncorrected *p* values, using two procedures. First, results were examined at $p < 0.001$, and then re-examined at a size-adjusted probability value to test whether lack of significant effects in the smallest group was a biological, rather than statistical, phenomenon. Only the MH group showed significant abnormalities at $p < 0.001$. At a size-adjusted *p* value, the PH group showed clusters of increased PiB retention compared to NH MCI, which supports the view that paternal transmission is also associated with amyloid deposition, albeit to a lesser degree than maternal transmission. While this procedure can only be regarded as descriptive, we offer that using both procedures would give a clearer picture of brain abnormalities across relatively small groups. The use of an adjusted *p* threshold may not fully protect against results due to chance, but it may be more suitable for clinical research with relatively small samples of patients than the more conservative $p < 0.001$ [52]. This type of more liberal threshold has been previously applied to resting-state imaging studies by several groups [31, 51–54].

Alternatively, it has been argued that attempts at adjusting for significance threshold by dividing by sample size may either unfairly penalize large samples or unfairly benefit small samples [84]. Should this be the case, our results would further indicate that maternal transmission of LOAD is strongly associated with brain abnormalities at the MCI stage of AD, whereas paternal transmission is not. Studies with larger samples are needed to validate present findings.

We caution that the MCI population selected in our study represents a group with a high *a priori* risk of AD, results were made with small numbers of subjects under controlled clinical conditions, and our observations are restricted to MCI with and without a family history of dementia. Replication of these preliminary research findings in community-based populations is warranted and clinical application is not justified. Nevertheless, we believe that present multi-modality PET and MRI results are plausible and promising, and set the stage for further studies of MCI at increased risk for AD with longitudinal follow-ups and larger samples.

ACKNOWLEDGMENTS

The authors are grateful to Dr. Ana Lukic for her assistance with image analysis. Data used in the preparation of this article were obtained from the Alzheimer's disease Neuroimaging Initiative (ADNI) database (<http://adni.loni.ucla.edu/>). As such, the investigators within the ADNI contributed to the design and implementation of ADNI and/or provided data but did not participate in analysis or writing of this report. ADNI investigators include (complete listing available at http://adni.loni.ucla.edu/wp-content/uploads/how_to_apply/ADNI_Acknowledgement_List.pdf).

Authors' disclosures available online (<http://www.jalz.com/disclosures/view.php?id=1667>).

REFERENCES

- [1] Petersen RC, Roberts RO, Knopman DS, Boeve BF, Geda YE, Ivnik RJ, Smith GE, Jack CR, Jr (2009) Mild cognitive impairment: Ten years later. *Arch Neurol* **66**, 1447-1455.
- [2] Petersen RC, Smith GE, Waring SC, Ivnik RJ, Tangalos EG, Kokmen E (1999) Mild cognitive impairment: Clinical characterization and outcome. *Arch Neurol* **56**, 303-308.
- [3] Cohen AD, Price JC, Weissfeld LA, James J, Rosario BL, Bi W, Nebes RD, Saxton JA, Snitz BE, Aizenstein HA, Wolk DA, Dekosky ST, Mathis CA, Klunk WE (2009) Basal cerebral metabolism may modulate the cognitive effects of Abeta in mild cognitive impairment: An example of brain reserve. *J Neurosci* **29**, 14770-14778.
- [4] Forsberg A, Engler H, Almkvist O, Blomquist G, Hagman G, Wall A, Ringheim A, Langstrom B, Nordberg A (2008) PET imaging of amyloid deposition in patients with mild cognitive impairment. *Neurobiol Aging* **29**, 1456-1465.
- [5] Jack CR Jr, Lowe VJ, Weigand SD, Wiste HJ, Senjem ML, Knopman DS, Shiung MM, Gunter JL, Boeve BF, Kemp BJ, Weiner M, Petersen RC (2009) Serial PIB and MRI in normal, mild cognitive impairment and Alzheimer's disease: Implications for sequence of pathological events in Alzheimer's disease. *Brain* **132**, 1355-1365.
- [6] Kemppainen NM, Aalto S, Wilson IA, Nagren K, Helin S, Bruck A, Oikonen V, Kailajarvi M, Scheinin M, Viitanen M, Parkkola R, Rinne JO (2007) PET amyloid ligand [11C]PIB uptake is increased in mild cognitive impairment. *Neurology* **68**, 1603-1606.
- [7] Li Y, Rinne JO, Mosconi L, Pirraglia E, Rusinek H, DeSanti S, Kemppainen N, Nagren K, Kim BC, Tsui W, de Leon MJ (2008) Regional analysis of FDG and PIB-PET images in normal aging, mild cognitive impairment, and Alzheimer's disease. *Eur J Nucl Med Mol Imaging* **35**, 2169-2181.
- [8] Lopresti BJ, Klunk WE, Mathis CA, Hoge JA, Ziolkowski SK, Lu X, Meltzer CC, Schimmel K, Tsopelas ND, DeKosky ST, Price JC (2005) Simplified quantification of Pittsburgh Compound B amyloid imaging PET studies: A comparative analysis. *J Nucl Med* **46**, 1959-1972.
- [9] Mormino EC, Kluth JT, Madison CM, Rabinovici GD, Baker SL, Miller BL, Koeppe RA, Mathis CA, Weiner MW, Jagust WJ (2009) Episodic memory loss is related to hippocampal-mediated beta-amyloid deposition in elderly subjects. *Brain* **132**, 1310-1323.
- [10] Klunk WE, Engler H, Nordberg A, Wang Y, Blomquist G, Holt DP, Bergstrom M, Savitcheva I, Huang GF, Estrada S, Ausen B, Debnath ML, Barletta J, Price JC, Sandell J, Lopresti BJ, Wall A, Koivisto P, Antoni G, Mathis CA, Langstrom B (2004) Imaging brain amyloid in Alzheimer's disease with Pittsburgh Compound-B. *Ann Neurol* **55**, 306-319.
- [11] Okello A, Koivunen J, Edison P, Archer HA, Turkheimer FE, Nagren K, Bullock R, Walker Z, Kennedy A, Fox NC, Rossor MN, Rinne JO, Brooks DJ (2009) Conversion of amyloid positive and negative MCI to AD over 3 years: An 11C-PIB PET study. *Neurology* **73**, 754-760.
- [12] Resnick SM, Sojkova J, Zhou Y, An Y, Ye W, Holt DP, Dannals RF, Mathis CA, Klunk WE, Ferrucci L, Kraut MA, Wong DF (2010) Longitudinal cognitive decline is associated with fibrillar amyloid-beta measured by [11C]PiB. *Neurology* **74**, 807-815.
- [13] Wolk DA, Price JC, Saxton JA, Snitz BE, James JA, Lopez OL, Aizenstein HJ, Cohen AD, Weissfeld LA, Mathis CA, Klunk WE, De-Kosky ST (2009) Amyloid imaging in mild cognitive impairment subtypes. *Ann Neurol* **65**, 557-568.
- [14] Morris JC, Roe CM, Grant EA, Head D, Storandt M, Goate AM, Fagan AM, Holtzman DM, Mintun MA (2009) Pittsburgh compound B imaging and prediction of progression from cognitive normality to symptomatic Alzheimer disease. *Arch Neurol* **66**, 1469-1475.
- [15] Herholz K, Salmon E, Perani D, Baron JC, Holthoff V, Frollich L, Schonknecht P, Ito K, Mielke R, Kalbe E, Zundorf G, Delbeuck X, Pelati O, Anchisi D, Fazio F, Kerrouche N, Desgranges B, Eustache F, Beuthien-Baumann B, Menzel C, Schroder J, Kato T, Arahata Y, Henze M, Heiss WD (2002) Discrimination between Alzheimer dementia and controls by automated analysis of multicenter FDG PET. *Neuroimage* **17**, 302-316.
- [16] Minoshima S, Giordani B, Berent S, Frey KA, Foster NL, Kuhl DE (1997) Metabolic reduction in the posterior cingulate

- cortex in very early Alzheimer's disease. *Ann Neurol* **42**, 85-94.
- [17] Mosconi L, Tsui WH, Herholz K, Pupi A, Drzezga A, Lucignani G, Reiman EM, Holthoff V, Kalbe E, Sorbi S, Diehl-Schmid J, Perneczky R, Clerici F, Caselli R, Beuthien-Baumann B, Kurz A, Minoshima S, de Leon MJ (2008) Multicenter standardized 18F-FDG PET diagnosis of mild cognitive impairment, Alzheimer's disease, and other dementias. *J Nucl Med* **49**, 390-398.
- [18] Nestor PJ, Fryer TD, Smielewski P, Hodges JR (2003) Limbic hypometabolism in Alzheimer's disease and mild cognitive impairment. *Ann Neurol* **54**, 343-351.
- [19] Drzezga A, Lautenschlager N, Siebner H, Riemenschneider M, Willoch F, Minoshima S, Schwaiger M, Kurz A (2003) Cerebral metabolic changes accompanying conversion of mild cognitive impairment into Alzheimer's disease: A PET follow-up study. *Eur J Nucl Med Mol Imaging* **30**, 1104-1113.
- [20] Mosconi L, Perani D, Sorbi S, Herholz K, Nacmias B, Holthoff V, Salmon E, Baron JC, De Cristofaro MT, Padovani A, Borroni B, Franceschi M, Bracco L, Pupi A (2004) MCI conversion to dementia and the APOE genotype: A prediction study with FDG-PET. *Neurology* **63**, 2332-2340.
- [21] De Santi S, de Leon MJ, Rusinek H, Convit A, Tarshish CY, Roche A, Tsui WH, Kandil E, Boppana M, Daisley K, Wang GJ, Schlyer D, Fowler J (2001) Hippocampal formation glucose metabolism and volume losses in MCI and AD. *Neurobiol Aging* **22**, 529-539.
- [22] Jack CR Jr, Petersen RC, Xu YC, O'Brien PC, Smith GE, Ivnik RJ, Boeve BF, Waring SC, Tangalos EG, Kokmen E (1999) Prediction of AD with MRI-based hippocampal volume in mild cognitive impairment. *Neurology* **52**, 1397-1403.
- [23] Jack CR Jr, Knopman DS, Jagust WJ, Shaw LM, Aisen PS, Weiner MW, Petersen RC, Trojanowski JQ (2010) Hypothetical model of dynamic biomarkers of the Alzheimer's pathological cascade. *Lancet Neurol* **9**, 119-128.
- [24] van de Pol LA, van der Flier WM, Korf ES, Fox NC, Barkhof F, Scheltens P (2007) Baseline predictors of rates of hippocampal atrophy in mild cognitive impairment. *Neurology* **69**, 1491-1497.
- [25] Blacker D, Tanzi RE (1998) The genetics of Alzheimer disease: Current status and future prospects. *Arch Neurol* **55**, 294-296.
- [26] Farrer LA, O'Sullivan DM, Cupples LA, Growdon JH, Myers RH (1989) Assessment of genetic risk for Alzheimer's disease among first-degree relatives. *Ann Neurol* **25**, 485-493.
- [27] Mosconi L, Berti V, Swerdlow RH, Pupi A, Duara R, de Leon M (2010) Maternal transmission of Alzheimer's disease: Prodromal metabolic phenotype and the search for genes. *Hum Genom* **4**, 170-193.
- [28] Honea RA, Swerdlow RH, Vidoni ED, Burns JM (2011) Progressive regional atrophy in normal adults with a maternal history of Alzheimer disease. *Neurology* **76**, 822-829.
- [29] Honea RA, Swerdlow RH, Vidoni ED, Goodwin J, Burns JM (2010) Reduced gray matter volume in normal adults with a maternal family history of Alzheimer disease. *Neurology* **74**, 113-120.
- [30] Mosconi L, Rinne JO, Tsui WH, Berti V, Li Y, Wang H, Murray J, Scheinin N, Nagren K, Williams S, Glodzik L, De Santi S, Vallabhajosula S, de Leon MJ (2010) Increased fibrillar amyloid-beta burden in normal individuals with a family history of late-onset Alzheimer's. *Proc Natl Acad Sci U S A* **107**, 5949-5954.
- [31] Mosconi L, Rinne JO, Tsui W, Murray J, Li Y, Glodzik L, McHugh P, Williams S, Cummings M, Pirraglia E, Goldsmith SJ, Vallabhajosula S, Scheinin N, Viljanen T, Nagren K, de Leon MJ (2013) Amyloid and metabolic PET imaging of cognitively normal adults with Alzheimer's parents. *Neurobiol Aging* **34**, 22-34.
- [32] Mosconi L, Mistur R, Switalski R, Brys M, Glodzik L, Rich K, Pirraglia E, Tsui W, De Santi S, de Leon MJ (2009) Declining brain glucose metabolism in normal individuals with a maternal history of Alzheimer disease. *Neurology* **72**, 513-520.
- [33] Mosconi L, Brys M, Switalski R, Mistur R, Glodzik L, Pirraglia E, Tsui W, De Santi S, de Leon MJ (2007) Maternal family history of Alzheimer's disease predisposes to reduced brain glucose metabolism. *Proc Natl Acad Sci U S A* **104**, 19067-19072.
- [34] Reiter K, Alpert KI, Cobia DJ, Kwasny MJ, Morris JC, Csernansky JC, Wang L (2012) Cognitively normal individuals with AD parents may be at risk for developing aging-related cortical thinning patterns characteristic of AD. *Neuroimage* **61**, 525-532.
- [35] Andrawis JP, Hwang KS, Green AE, Kotlerman J, Elashoff D, Morra JH, Cummings JL, Toga AW, Thompson PM, Apostolova LG (2012) Effects of ApoE4 and maternal history of dementia on hippocampal atrophy. *Neurobiol Aging* **33**, 856-866.
- [36] Petersen RC, Aisen PS, Beckett LA, Donohue MC, Gamst AC, Harvey DJ, Jack CR Jr, Jagust WJ, Shaw LM, Toga AW, Trojanowski JQ, Weiner MW (2010) Alzheimer's Disease Neuroimaging Initiative (ADNI): Clinical characterization. *Neurology* **74**, 201-209.
- [37] Folstein MF, Folstein SE, McHugh PR (1975) "Mini-mental state". A practical method for grading the cognitive state of patients for the clinician. *J Psychiatr Res* **12**, 189-198.
- [38] Morris JC (1993) The Clinical Dementia Rating (CDR): Current version and scoring rules. *Neurology* **43**, 2412-2414.
- [39] McKhann G, Drachman D, Folstein M, Katzman R, Price D, Stadlan EM (1984) Clinical diagnosis of Alzheimer's disease: Report of the NINCDS-ADRDA Work Group under the auspices of Department of Health and Human Services Task Force on Alzheimer's Disease. *Neurology* **34**, 939-944.
- [40] Mathis CA, Wang Y, Holt DP, Huang GF, Debnath ML, Klunk WE (2003) Synthesis and evaluation of 11C-labeled 6-substituted 2-arylbenzothiazoles as amyloid imaging agents. *J Med Chem* **46**, 2740-2754.
- [41] Joshi A, Koeppe RA, Fessler JA (2009) Reducing between scanner differences in multi-center PET studies. *Neuroimage* **46**, 154-159.
- [42] Ashburner J, Friston KJ (2000) Voxel-based morphometry—the methods. *Neuroimage* **11**, 805-821.
- [43] Ashburner J (2007) A fast diffeomorphic image registration algorithm. *Neuroimage* **38**, 95-113.
- [44] Price JC, Klunk WE, Lopresti BJ, Lu X, Hoge JA, Ziolkowski SK, Holt DP, Meltzer CC, DeKosky ST, Mathis CA (2005) Kinetic modeling of amyloid binding in humans using PET imaging and Pittsburgh Compound-B. *J Cereb Blood Flow Metab* **25**, 1528-1547.
- [45] Muller-Gartner HW, Links JM, Prince JL, Bryan RN, McVeigh E, Leal JP, Davatzikos C, Frost JJ (1992) Measurement of radiotracer concentration in brain gray matter using positron emission tomography: MRI-based correction for partial volume effects. *J Cereb Blood Flow Metab* **12**, 571-583.

- [46] Meltzer CC, Leal JP, Mayberg HS, Wagner HNJr, Frost JJ (1990) Correction of PET data for partial volume effects in human cerebral cortex by MR imaging. *J Comput Assist Tomogr* **14**, 561-570.
- [47] Friston KJ, Frith CD, Liddle PF, Frackowiak RS (1991) Comparing functional (PET) images: The assessment of significant change. *J Cereb Blood Flow Metab* **11**, 690-699.
- [48] Chetelat G, Desgranges B, Landeau B, Mezenge F, Poline JB, de la Sayette V, Viader F, Eustache F, Baron JC (2008) Direct voxel-based comparison between grey matter hypometabolism and atrophy in Alzheimer's disease. *Brain* **131**, 60-71.
- [49] Berti V, Mosconi L, Glodzik L, Li Y, Murray J, De Santi S, Pupi A, Tsui W, De Leon MJ (2011) Structural brain changes in normal individuals with a maternal history of Alzheimer's. *Neurobiol Aging* **32**, 2325.e17-26.
- [50] Chetelat G, Desgranges B, de la Sayette V, Viader F, Eustache F, Baron JC (2003) Mild cognitive impairment: Can FDG-PET predict who is to rapidly convert to Alzheimer's disease? *Neurology* **60**, 1374-1377.
- [51] Chetelat G, Desgranges B, de la Sayette V, Viader F, Berkouk K, Landeau B, Lalevee C, Le Doze F, Dupuy B, Hannequin D, Baron JC, Eustache F (2003) Dissociating atrophy and hypometabolism impact on episodic memory in mild cognitive impairment. *Brain* **126**, 1955-1967.
- [52] Desgranges B, Baron JC, de la Sayette V, Petit-Taboué MC, Benali K, Landeau B, Lechevalier B, Eustache F (1998) The neural substrates of memory systems impairment in Alzheimer's disease. A PET study of resting brain glucose utilization. *Brain* **121**(Pt 4), 611-631.
- [53] Grasby PM, Frith CD, Friston KJ, Bench C, Frackowiak RS, Dolan RJ (1993) Functional mapping of brain areas implicated in auditory-verbal memory function. *Brain* **116**(Pt 1), 1-20.
- [54] O'Brien JT, Eagger S, Syed GM, Sahakian BJ, Levy R (1992) A study of regional cerebral blood flow and cognitive performance in Alzheimer's disease. *J Neurol Neurosurg Psychiatry* **55**, 1182-1187.
- [55] Braak H, Braak E (1991) Neuropathological staging of Alzheimer-related changes. *Acta Neuropathol* **82**, 239-259.
- [56] Braak H, Braak E, Bohl J, Reintjes R (1996) Age, neurofibrillary changes, A beta-amyloid and the onset of Alzheimer's disease. *Neurosci Lett* **210**, 87-90.
- [57] Haass C, Selkoe DJ (2007) Soluble protein oligomers in neurodegeneration: Lessons from the Alzheimer's amyloid beta-peptide. *Nat Rev Mol Cell Biol* **8**, 101-112.
- [58] Mosconi L, Sorbi S, de Leon MJ, Li Y, Nacmias B, Myoung PS, Tsui W, Ginestroni A, Bessi V, Fayyazz M, Caffarra P, Pupi A (2006) Hypometabolism exceeds atrophy in presymptomatic early-onset familial Alzheimer's disease. *J Nucl Med* **47**, 1778-1786.
- [59] Bobinski M, de Leon MJ, Wegiel J, Desanti S, Convit A, Saint Louis LA, Rusinek H, Wisniewski HM (2000) The histological validation of post mortem magnetic resonance imaging-determined hippocampal volume in Alzheimer's disease. *Neuroscience* **95**, 721-725.
- [60] Sokoloff L, Reivich M, Kennedy C, Des Rosiers MH, Patlak CS, Pettigrew KD, Sakurada O, Shinohara M (1977) The [¹⁴C]deoxyglucose method for the measurement of local cerebral glucose utilization: Theory, procedure, and normal values in the conscious and anesthetized albino rat. *J Neurochem* **28**, 897-916.
- [61] Drzezga A, Becker JA, Van Dijk KR, Sreenivasan A, Talukdar T, Sullivan C, Schultz AP, Sepulcre J, Putcha D, Greve D, Johnson KA, Sperling RA (2011) Neuronal dysfunction and disconnection of cortical hubs in non-demented subjects with elevated amyloid burden. *Brain* **134**, 1635-1646.
- [62] Meguro K, Blaizot X, Kondoh Y, Le Mestric C, Baron JC, Chavoix C (1999) Neocortical and hippocampal glucose hypometabolism following neurotoxic lesions of the entorhinal and perirhinal cortices in the non-human primate as shown by PET. Implications for Alzheimer's disease. *Brain* **122**(Pt 8), 1519-1531.
- [63] Engler H, Forsberg A, Almkvist O, Blomquist G, Larsson E, Savitcheva I, Wall A, Ringheim A, Langstrom B, Nordberg A (2006) Two-year follow-up of amyloid deposition in patients with Alzheimer's disease. *Brain* **129**, 2856-2866.
- [64] Edison P, Archer HA, Hinz R, Hammers A, Pavese N, Tai YF, Hotton G, Cutler D, Fox N, Kennedy A, Rossor M, Brooks DJ (2007) Amyloid, hypometabolism, and cognition in Alzheimer disease: An [¹¹C]PIB and [¹⁸F]FDG PET study. *Neurology* **68**, 501-508.
- [65] Frisoni GB, Lorenzi M, Caroli A, Kemppainen N, Nagren K, Rinne JO (2009) *In vivo* mapping of amyloid toxicity in Alzheimer disease. *Neurology* **72**, 1504-1511.
- [66] Green RC, Cupples LA, Go R, Benke KS, Edeki T, Griffith PA, Williams M, Hipps Y, Graff-Radford N, Bachman D, Farrer LA (2002) Risk of dementia among white and African American relatives of patients with Alzheimer disease. *JAMA* **287**, 329-336.
- [67] Cupples LA, Farrer LA, Sadovnick AD, Relkin N, Whitehouse P, Green RC (2004) Estimating risk curves for first-degree relatives of patients with Alzheimer's disease: The REVEAL study. *Genet Med* **6**, 192-196.
- [68] Silverman JM, Ciresi G, Smith CJ, Marin DB, Schnaider-Beerli M (2005) Variability of familial risk of Alzheimer disease across the late life span. *Arch Gen Psychiatry* **62**, 565-573.
- [69] Bennett DA, Schneider JA, Arvanitakis Z, Kelly JF, Aggarwal NT, Shah RC, Wilson RS (2006) Neuropathology of older persons without cognitive impairment from two community-based studies. *Neurology* **66**, 1837-1844.
- [70] Price JL, Morris JC (1999) Tangles and plaques in nondemented aging and "preclinical" Alzheimer's disease. *Ann Neurol* **45**, 358-368.
- [71] Terry RD, Masliah E, Salmon DP, Butters N, DeTeresa R, Hill R, Hansen LA, Katzman R (1991) Physical basis of cognitive alterations in Alzheimer's disease: Synapse loss is the major correlate of cognitive impairment. *Ann Neurol* **30**, 572-580.
- [72] Jagust WJ, Landau SM, Shaw LM, Trojanowski JQ, Koeppe RA, Reiman EM, Foster NL, Petersen RC, Weiner MW, Price JC, Mathis CA (2009) Relationships between biomarkers in aging and dementia. *Neurology* **73**, 1193-1199.
- [73] Furst AJ, Rabinovici GD, Rostomian AH, Steed T, Alkalay A, Racine C, Miller BL, Jagust WJ (2012) Cognition, glucose metabolism and amyloid burden in Alzheimer's disease. *Neurobiol Aging* **33**, 215-225.
- [74] Rabinovici GD, Furst AJ, Alkalay A, Racine CA, O'Neil JP, Janabi M, Baker SL, Agarwal N, Bonasera SJ, Mormino EC, Weiner MW, Gorno-Tempini ML, Rosen HJ, Miller BL, Jagust WJ (2010) Increased metabolic vulnerability in early-onset Alzheimer's disease is not related to amyloid burden. *Brain* **133**, 512-528.
- [75] Mosconi L, Berti V, Glodzik L, Pupi A, De Santi S, de Leon MJ (2010) Pre-clinical detection of Alzheimer's disease using FDG-PET, with or without amyloid imaging. *J Alzheimers Dis* **20**, 843-854.
- [76] Debette S, Wolf PA, Beiser A, Au R, Himali JJ, Pikula A, Auerbach S, Decarli C, Seshadri S (2009) Association of

- parental dementia with cognitive and brain MRI measures in middle-aged adults. *Neurology* **73**, 2071-2078.
- [77] Duara R, Barker WW, Lopez-Alberola R, Loewenstein DA, Grau LB, Gilchrist D, Sevush S, St George-Hyslop S (1996) Alzheimer's disease: Interaction of apolipoprotein E genotype, family history of dementia, gender, education, ethnicity, and age of onset. *Neurology* **46**, 1575-1579.
- [78] Edland SD, Silverman JM, Peskind ER, Tsuang D, Wijsman E, Morris JC (1996) Increased risk of dementia in mothers of Alzheimer's disease cases: Evidence for maternal inheritance. *Neurology* **47**, 254-256.
- [79] Gomez-Tortosa E, Barquero MS, Baron M, Sainz MJ, Manzano S, Payno M, Ros R, Almaraz C, Gomez-Garre P, Jimenez-Escrig A (2007) Variability of age at onset in siblings with familial Alzheimer disease. *Arch Neurol* **64**, 1743-1748.
- [80] Bendlin BB, Ries ML, Canu E, Sodhi A, Lazar M, Alexander AL, Carlsson CM, Sager MA, Asthana S, Johnson SC (2010) White matter is altered with parental family history of Alzheimer's disease. *Alzheimers Dement* **6**, 394-403.
- [81] Mosconi L, Glodzik L, Mistur R, McHugh P, Rich KE, Javier E, Williams S, Pirraglia E, De Santi S, Mehta PD, Zinkowski R, Blennow K, Pratico D, de Leon MJ (2010) Oxidative stress and amyloid-beta pathology in normal individuals with a maternal history of Alzheimer's. *Biol Psychiatry* **68**, 913-921.
- [82] Lin MT, Beal MF (2006) Mitochondrial dysfunction and oxidative stress in neurodegenerative diseases. *Nature* **443**, 787-795.
- [83] Kawas C, Segal J, Stewart WF, Corrada M, Thal LJ (1994) A validation study of the Dementia Questionnaire. *Arch Neurol* **51**, 901-906.
- [84] Witte JS, Elston RC, Cardon LR (2000) On the relative sample size required for multiple comparisons. *Stat Med* **19**, 369-372.